

## Propagation of the preliminary reverse impulse of sudden commencements to low latitudes

P. J. Chi,<sup>1</sup> C. T. Russell,<sup>1</sup> J. Raeder,<sup>1</sup> E. Zesta,<sup>2</sup> K. Yumoto,<sup>3</sup> H. Kawano,<sup>3</sup> K. Kitamura,<sup>3</sup> S. M. Petrinec,<sup>4</sup> V. Angelopoulos,<sup>5</sup> G. Le,<sup>6</sup> and M. B. Moldwin<sup>1</sup>

**Abstract.** It has been thought that the preliminary reverse impulse (PRI) of the sudden commencements (SC) phenomena occurs simultaneously on the ground at different locations. A popular explanation is that the PRI propagates through the Earth-ionosphere waveguide at the 35 ground magnetometer stations during the SC event on September 24, 1998, and found clear differences in the arrival time of PRI. We calculated the MHD wave propagation time from the location of the first compression of the magnetosphere to the low-latitude ground stations and found good agreement with the observed PRI arrival times. Our calculation also indicates that the wavefront is seriously distorted by the inhomogeneity of the magnetosphere and the small difference in PRI arrival time between high-latitude and low-latitude observations cannot be an indicator of a super-Alfvénic propagation. We also found implications that high-latitude PRIs can be induced by the vortex of ionospheric currents at nearby latitudes, and the motion of the current vortex can affect the arrival time of high-latitude PRIs.

### 1. Introduction

A sudden commencement (SC) is a unique and clear phenomenon in the magnetosphere when the system reacts in response to an interplanetary shock or discontinuity originating from the Sun. Among a variety of perturbations in the solar wind, this type of discontinuity delivers the most severe enhancement to the solar wind dynamic pressure. Since the balance in dynamic pressure determines the shape of the magnetosphere, these interplanetary shocks or discontinuities create one of the most dramatic changes of the magnetospheric configuration. Therefore the consequent SC is a natural experimental setup to study how the magnetosphere reacts to solar wind variations.

Besides a simple step-like increase in the geomagnetic field due to the compression of the magnetosphere, a complicated SC structure is usually found in ground magnetic field records. Important characteristics of SC have been identified during the International Geophysical Year (IGY) era [e.g., *Matsushita*, 1962]. In particular, a class of SC, denoted as  $\bar{SC}$  or  $SC^*$ , is characterized by a negative impulse in the  $H$  component preceding the positive main impulse. It was soon realized that the preliminary impulse (PI, or the preliminary reverse impulse, PRI) and the main impulse (MI) correspond to two different driving mechanisms. *Nishida* [1964] and *Tamao* [1964a] independently

interpreted the PRI as a signature of ionospheric Hall currents at high latitudes caused by the incidence of transverse hydromagnetic waves. These waves are produced by the compression of the magnetosphere in the subsolar region at the very beginning of the SC. *Araki* [1977] indicated that the MI should contain  $DL_{MI}$ , the disturbance caused by an abrupt increase of the magnetopause current and the ensuing ring current and tail current, and  $DP_{MI}$ , the variation due to a polar electric field transmitted along lines of force from the upper magnetosphere. The superposition of these two MI fields is similar to what *Obayashi and Jacobs* [1957] suggested in a mathematical model.

The Nishida-Tamao model nicely explains the major features of PRI seen in observations. When MHD waves propagate in a three-dimensional space from a point source, the mixture of the fast mode and the converted Alfvén mode results in a twin-vortex pattern of streamlines [*Tamao*, 1964b]. Consequently, a similar twin-vortex structure of Hall currents is formed in the ionosphere. *Lysak and Lee* [1992] have confirmed such vortex structure in their simulation. In the Northern Hemisphere the vortex is counterclockwise in the morning and clockwise in the afternoon, and the corresponding magnetic field in the  $H$  component increases and decreases, respectively. Therefore a PRI tends to occur in the afternoon side, and the positive PI in the morning sector cannot be seen easily because it has the same sense as the succeeding MI signal.

While the picture that the source of PRI is Alfvén waves generated by the compression of the magnetosphere is not controversial, how the signal propagates to different ground locations around the globe has been less certain. A popular interpretation at this moment is that the electric field, driven by the Alfvénic waves and confined in the polar region, propagates through the space between the ionosphere and the ground at a super-Alfvénic speed to low-latitude regions and the equator, as proposed first in the classic work by *Araki* [1977]. This model was later supported by *Kikuchi and Araki* [1979a, 1979b], who confirmed the existence of the zeroth-order TM mode in the Earth-ionosphere waveguide.

An important motivation behind the model of waveguide propagation at the speed of light is the simultaneous observation of PRI seen at both high latitudes and the equatorial region [e.g.,

<sup>1</sup>Institute of Geophysics and Planetary Physics, University of California, Los Angeles, California, USA.

<sup>2</sup>Department of Atmospheric Sciences, University of California, Los Angeles, California, USA.

<sup>3</sup>Department of Earth and Planetary Sciences, Kyushu University, Fukuoka, Japan.

<sup>4</sup>Lockheed Martin Advanced Technology Center, Palo Alto, California, USA.

<sup>5</sup>Space Science Laboratory, University of California, Berkeley, California, USA.

<sup>6</sup>Goddard Space Flight Center, NASA Greenbelt, Maryland, USA.

Araki, 1977; Kikuchi and Araki, 1979a, 1979b]. However, as the timing resolution of magnetometers has improved in recent years, some studies have shown small differences in time of the PRI signals at different stations [Petrinec et al., 1996; Yumoto et al., 1997; Engebretson et al., 1999]. Questions have been raised regarding the validity of the waveguide propagation model [Yumoto et al., 1997].

In this study, we present tangible evidence that the arrival time of the low-latitude PRI recorded by accurately synchronized magnetometers can be well explained by the MHD wave propagation model. The unambiguous difference in the observed PRI arrival times also reveals disagreement with the picture of waveguide propagation. Our observations are based on the SC event on September 24, 1998, from 35 magnetometer stations on the American continents and in the West Pacific regions. In our discussion of the MHD wave propagation we first demonstrate the essential features of signal propagation in a dipole magnetosphere, and then use the Tsyganenko 1996 magnetospheric field model for the comparison between data and theory.

## 2. Observations

At 2345 UT on September 24, 1998, the magnetosphere was suddenly compressed as the dynamic pressure of the solar wind rapidly rose. The solar wind velocity suddenly increased from 400 to over 600 km/s and the density jumped from 8 to over 20  $\text{cm}^{-3}$  causing an increase in the dynamic pressure from 2 to 15 nPa. The interplanetary magnetic field (IMF) was strong and in

the positive  $Y$ -GSM direction throughout [Russell et al., 1999]. Selected as an International Solar Terrestrial Physics (ISTP) Event and a Global Environment Modeling (GEM) Storm Event, the interval from September 23 to 26, 1998, has been studied from a wide range of perspectives from the preceding interplanetary shock, the outflows from the ionosphere, to the succeeding magnetic storm [e.g., Moore et al., 1999; Russell et al., 1999, 2000; Strangeway et al., 2000; Chi et al., 2000]. In particular, the sudden compression in magnetic field observed by the Polar and GOES spacecraft is described by Russell et al. [1999] in detail. The strong and step-like increase in solar wind dynamic pressure makes this event a classical SC to study.

The 35 stations belong to several magnetometer networks: The MACCS array is located at the cusp latitudes in northern Canada [Hughes and Engebretson, 1997]; the CANOPUS magnetometer array covers the auroral and subauroral regions in Canada; UCLA built four U.S. magnetometers, for which the Florida Tech (FIT) station is the first MEASURE magnetometer and the other three belong to the IGPP/LANL array; the CPMN network consists of stations in Asian countries, Australia, and South America [Yumoto and the 210 MM Magnetic Observation Group, 1996]. All 35 stations recorded clear signatures of the SC event on September 24, 1998. The locations of these stations are illustrated in Figure 1, in which solid and open circles indicate the stations that saw and did not see the PRI, respectively. The occurrence of PRI in the afternoon sector is consistent with the twin-vortex pattern discussed earlier.

The timing resolution and accuracy of magnetometers are top instrument requirements for the data analysis of PRI. All the

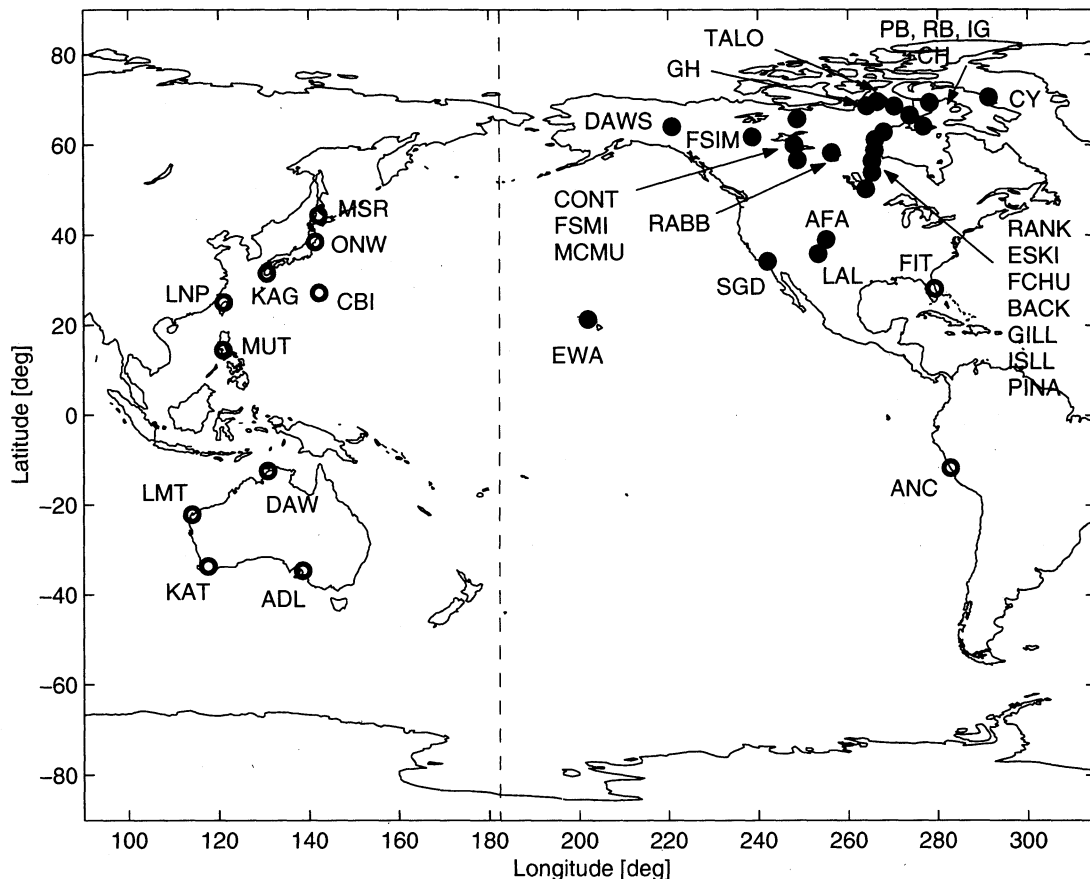


**Figure 1.** Map of the locations in geographic coordinates of 35 magnetometers, including stations of CANOPUS, CPMN, IGPP/LANL, and MACCS arrays. Solid (open) circles represent the stations that saw (did not see) PRI signals during the SC event on September 24, 1998. The dashed line at 182° longitude represents the local noon at the time of the SC.

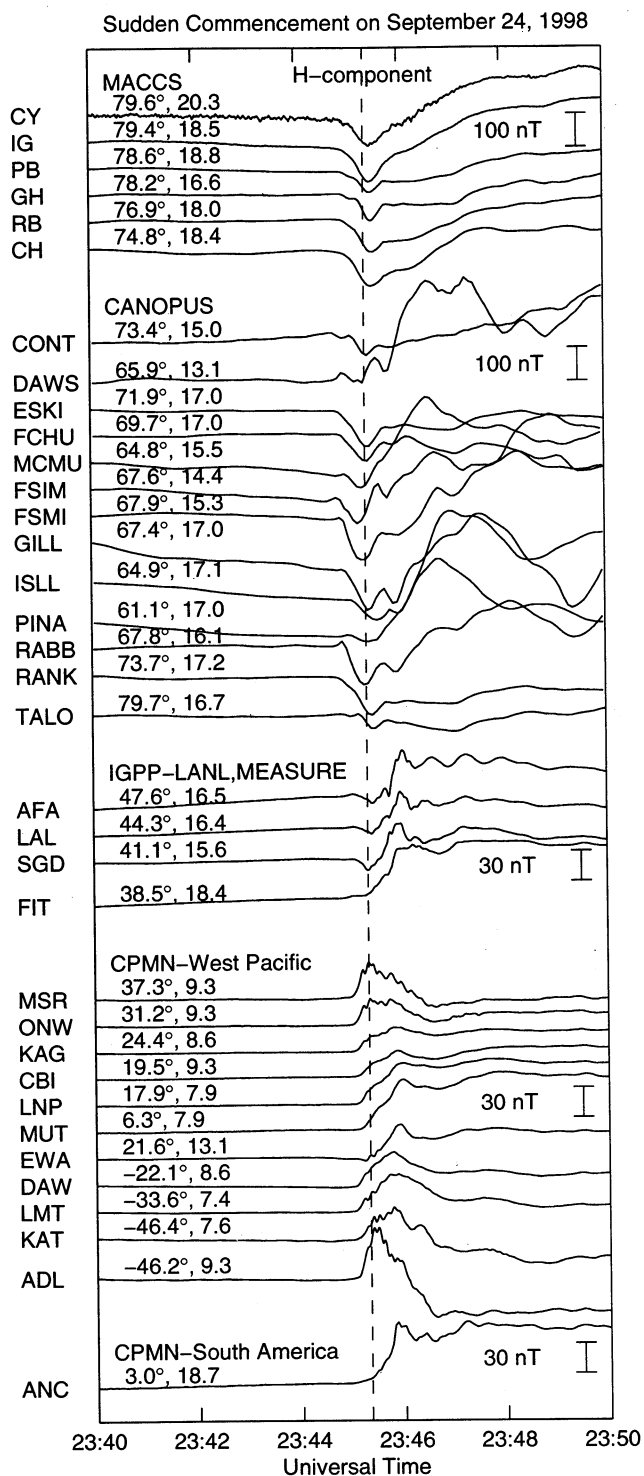


**Figure 2.** Time series of magnetic field in the  $H$  component recorded by the thirty-five stations studied in this study. The two numbers on the top of each trace are the magnetic latitude and magnetic local time of the station when the SC occurred. The dashed vertical line is plotted at 2345:20 UT as a reference time.

stations included in this study have time resolution not lower than 5 s, which is adequate to identify the PRI phenomenon that lasts for an order of 1 min. The IGPP/LANL stations and some CPMN stations have time resolution of 1 s, and they are synchronized by the Global Positioning System (GPS) signals. MACCS and CANOPUS stations do not use GPS timing, although MACCS data have a finer time resolution at 0.5 s.

Figure 2 shows 10 min of magnetometer data, centered roughly at the time of the SC, from the 35 stations. The station location in magnetic latitude and magnetic local time is also shown in Figure 2 as a convenient reference. The MACCS stations and many CANOPUS stations saw PRI signals with amplitudes of order 100 nT in the  $H$  component. The PRI tended to be weaker at lower latitudes except what was observed at TALO, located at the highest magnetic latitude at 79.7°. The amplitude of PRI dropped to ~10 nT at the three IGPP/LANL stations. The only CPMN station that observed PRI is EWA, which was located in the afternoon sector. The dashed vertical line at the center of the Figure is plotted at 2345:20 UT as a reference time when many stations observed PRI. However, the time when the minimum value of  $B_H$  was recorded varies from station to station, and we will discuss the details of the PRI arrival time in section 3.

The CPMN stations in Asian regions were in the morning sector, and they did not observe any PRI signal as expected. Nevertheless, their data seem to indicate a bulge in  $B_H$  before the main impulse reached its peak, consistent with the model of ionospheric twin vortices. In Australia the northern two stations showed a similar pattern as what was observed in the Northern Hemisphere. The southern two stations had positive impulses in  $B_H$  before the main impulse coming afterward, and these preliminary impulses are consistent with the same model of the ionospheric vortices but in the Southern Hemisphere. Located in the nightside at the time of the SC event, ANC (South America) and FIT (United States) did not observe PRI.

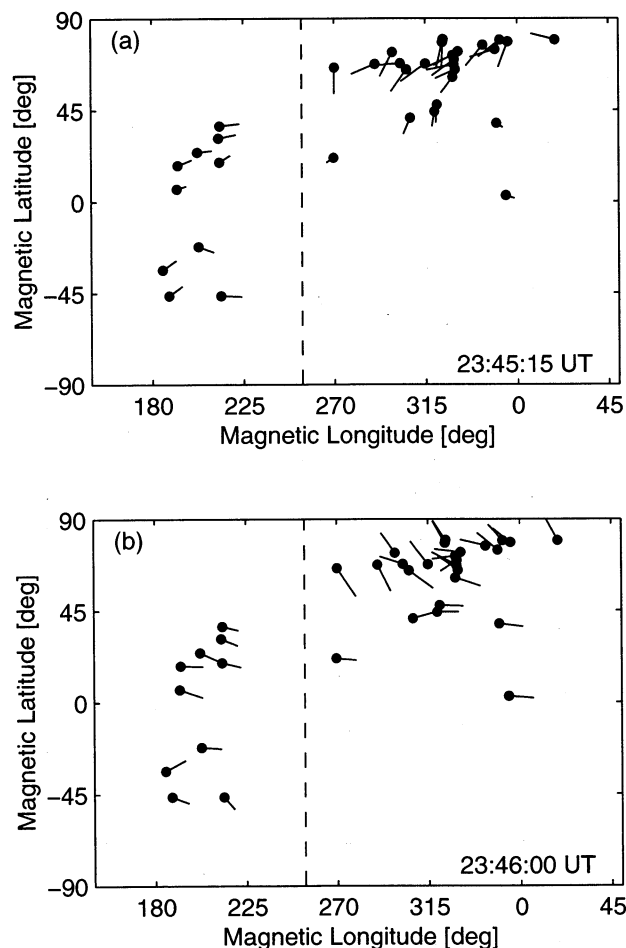


**Figure 3.** Ionospheric equivalent currents at the times of (a) PI and (b) MI. The vertical dashed lines indicate the locations of magnetic local noon.

Plots of ionospheric equivalent currents are useful to understand the current system that drives SC, although these plotted vectors also contain the effects of magnetospheric currents. Figure 3 shows the equivalent ionospheric currents derived from the magnetic field perturbations in the  $H$  and  $D$  components at 2345:15 UT and 2346:00 UT, representing the times when PRI and MI signals were dominant, respectively. In order to see both the strong PRI at high latitudes and the much weaker PRI at lower latitudes in the same plot, we make each vector length proportional to the logarithm of its magnitude. In Figure 3a all equivalent current vectors in the morning sector are directed toward noon, signaling increases in  $B_H$  on the ground. Most vectors in the afternoon side are also directed toward noon, indicating decreases in  $B_H$  as the PRI signature. These facts are consistent with the ionospheric twin-vortex structure suggested by *Tamao* [1964a] if we imagine that the center of the afternoon vortex was located at a higher latitude relative to the stations in Canada and United States. The pattern in Figure 3b shows eastward currents at the middle and low latitudes and reverse currents flowing at higher latitudes. This pattern can be understood as a superposition of the  $DL_{MI}$ , which is more important at low latitudes, and the  $DP_{MI}$ , the twin-vortex currents with an opposite sense to the preceding one associated with PI.

### 3. Propagation of PRI

There are two speeds relevant to the propagation of PRI in existing theories: One is the zeroth-order TM mode propagating along the Earth-ionosphere cavity approximately at the speed of light [Kikuchi and Araki, 1979b], and the other is the MHD wave propagation at speeds of the fast mode and the Alfvén mode [Tamao, 1964a]. In the former case the propagation time from high-latitude regions to low latitudes or the equator is negligibly short ( $\leq 0.03$  s), so the signals at all locations should occur simultaneously. In comparison, MHD waves travel much more slowly, and their propagation time will be discussed here in detail.

*Tamao* [1964b] depicts a picture of MHD wave propagation from a source to an observer on the ground (see Figure 4). When waves are generated from a point source  $Q$ , compressional waves are launched from the source to all directions, in addition to the Alfvén wave traveling along the field line. The amplitude of the compressional waves suffers a geometrical attenuation proportional to  $R^{-1}$ , where  $R$  is the distance from the source. Owing to the inhomogeneity of the Alfvén speed in the magnetosphere, the compressional mode converts to the Alfvén mode everywhere in space. Provided that there is no other wave present in the system, two kinds of waves can be seen by a ground observer at  $P$ : the compressional (fast) mode wave that comes directly from the source and the Alfvén waves converted from the fast mode everywhere on the field line connected to  $P$ . We can assume that the converted Alfvén waves can travel without any attenuation because their wave energy is guided along the magnetic field. Therefore the strongest wave reaching the ground observer  $P$  would be the one traveling along the path,  $\widehat{QP_0-P_0P}$ , which consists of a straight-line path from  $Q$  to  $P_0$  and then the path from  $P_0$  to  $P$  along the field line, since  $\widehat{QP_0}$  is the shortest path from the source to the field line of consideration. In addition, owing to the different traveling paths, these waves do not arrive on the ground at the same time. For example,  $\widehat{QP_4-P_4P}$  should be a faster route than  $\widehat{QP_0-P_0P}$  since  $\widehat{QP_4}$  is shorter than  $\widehat{QP_0-P_0P_4}$  and since the fast mode speed and the Alfvén speed are equal if the plasma is assumed to be cold. An extreme case of propagation paths is the straight-line path  $\widehat{QP}$ , by which the wave can reach  $P$  the soonest but suffers the greatest attenuation. Having all these considerations, we can imagine that the ground observer  $P$  sees a temporal variation of the magnetic field as shown in the inset in Figure 4.

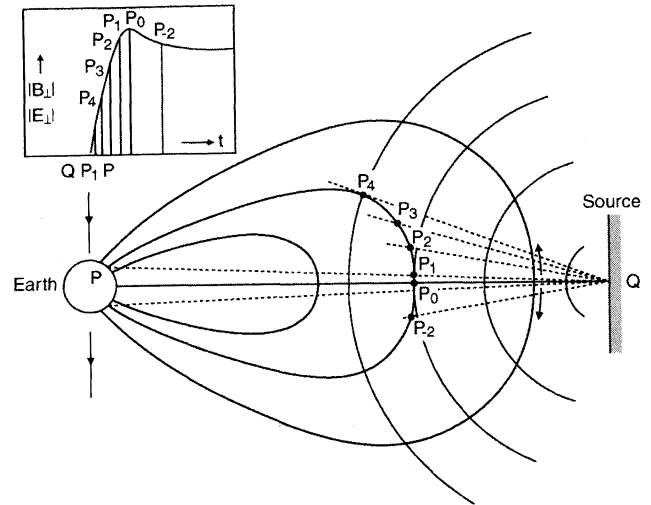


**Figure 4.** Schematic illustration of the propagation of MHD waves from a point source  $Q$  to a ground observer  $P$ . In addition to the compressional (fast) mode wave directly from the source, the observer  $P$  also sees Alfvén waves converted from the fast mode everywhere along the field line such as  $P_{-2}$ ,  $P_0$ ,  $P_1$ , etc. The inset shows the temporal variation of  $B_H$  at  $P$  [After *Tamao*, 1964b].

In order to understand the essential features of the propagation time of the MHD waves in the magnetosphere, we began by calculating the travel time in a dipole magnetic field, in which  $|\mathbf{B}| = (B_0 R_E^3 / r^3)(1 + 3\sin^2\theta)^{1/2}$ , where  $B_0 = 31,000$  nT and  $\theta$  is the magnetic latitude. For the plasma mass density we used a power law model as of *Lee and Lysak* [1989]:

$$n(r) = \begin{cases} n_{mp} \left( \frac{r_{mp}}{r} \right)^3, & r > 5 \\ n_{pp} \left( \frac{r_{pp}}{r} \right)^3, & r \leq 5 \end{cases} \quad (1)$$

where  $n_{mp} = 1$  amu/cm<sup>3</sup>,  $r_{mp} = 10 R_E$ ,  $n_{pp} = 150$  amu/cm<sup>3</sup>, and  $r_{pp} = 5 R_E$ . We also assume that the plasma is cold, which makes the fast mode speed equal to the Alfvén speed. The source is considered to be located at the equator at  $L = 10$  and the imaginary observatories located at different  $L$  values on the same meridian. For each different  $L$  value, we calculated the propagation time for the path as  $\widehat{QP_0-P_0P}$  in Figure 4. The wave traveling along such path is expected to produce the strongest signal on the ground.

Figure 5 presents the result of the calculation, including the propagation times of the fast mode and the Alfvén mode, and the sum of the two. The fast mode wave propagates along a radially inward path, and the propagation time increases as the wave travels closer to the Earth. The path of the Alfvén wave propagation is the longest at  $L = 10$  and smaller at lower  $L$  values, but the propagation time does not always decrease with decreasing  $L$ : It changes abruptly from 10 s for the field line immediately outside the plasmapause to 43 s for the one inside the plasmasphere where the density is much greater. As a result, the total travel time has a zigzag shape owing to the propagation along the magnetic field.

Although the exact values of propagation time contours may be different in a more realistic magnetosphere, Figure 5 suggests several interesting points relevant to the arrival time of the PRI observed by ground stations. First, the PRI signal tends to arrive

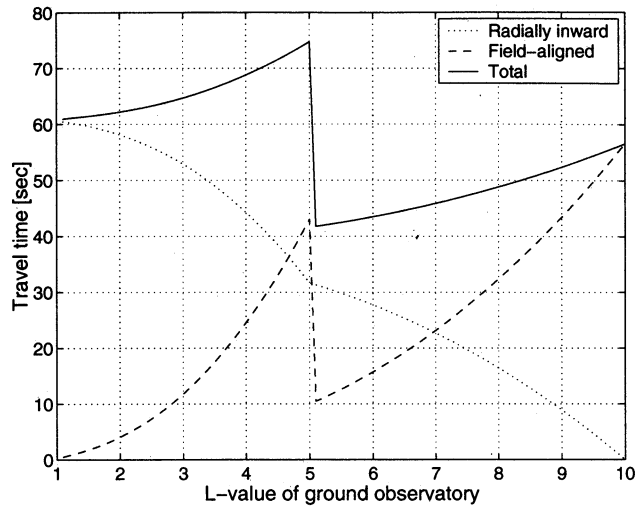


**Figure 5.** Travel time of MHD waves from a point source at  $L=10$  at the equator to ground observatories at different  $L$  values. The total travel time consists of the time from the source to the field line on the equator (dotted line) and the time from the equator to the ground along the magnetic field (dashed line).

sooner at a lower-latitude station than at a higher-latitude station, if field lines from both stations map to the same magnetospheric region, either the plasmasphere or the outer magnetosphere. The ground station located immediately outside the plasmapause latitude may observe the first PRI signal. Second, the difference of the PRI arrival time should be discernible if the magnetometers have high time resolution and accurate synchronization.

Magnetometers with a coarse time resolution, like 15 s data used by the SC studies in the 1970s and 1980s, may not be able to distinguish such fine differences. Third, the PRI arrival times at a high-latitude station and at the equator may be very similar, although the propagation speed is not super-Alfvénic.

In order to be consistent with our calculation of the PRI travel time, we assigned the time when the strongest PRI signal (i.e., the minimum in  $B_H$ ) is seen as the PRI arrival time. This definition also makes the identification of the PRI arrival time in geomagnetic field records easier since the inflection point, often used as an indicator of the PRI onset, is usually ill-defined. Figure 6 plots the arrival times of the PRI observed by 23 stations with respect to their locations in magnetic local time and magnetic latitude. The distinction among the arrival times clearly indicates that PRI did not occur simultaneously at all locations. The distribution of these arrival times also follows the trend suggested in Figure 5 that PRI arrives earlier at the mid-latitude stations outside the plasmapause latitude and at low-latitude stations. In addition, Figure 6 also suggests that the stations farther from the first compression at 12.3 MLT saw PRI later, possibly due to longer travel distances of the signal.

Some uncertainties exist in Figure 6 due to the inconsistent time resolution and uncertain synchronization across different magnetometer arrays. The three IGPP/LANL stations and the EWA station of CPMN all have 1-s time resolution, and they are synchronized by GPS signals. Therefore their PRI arrival times provide the most confident results. The 5-s CANOPUS data (for the points between  $61^\circ$  and  $74^\circ$  magnetic latitudes in Figure 6) contain much greater error bars in their results. All MACCS stations have 0.5-s time resolution so the determination of PRI arrival time should have smallest errors. However, they do not have common synchronization with IGPP/LANL and CPMN arrays.

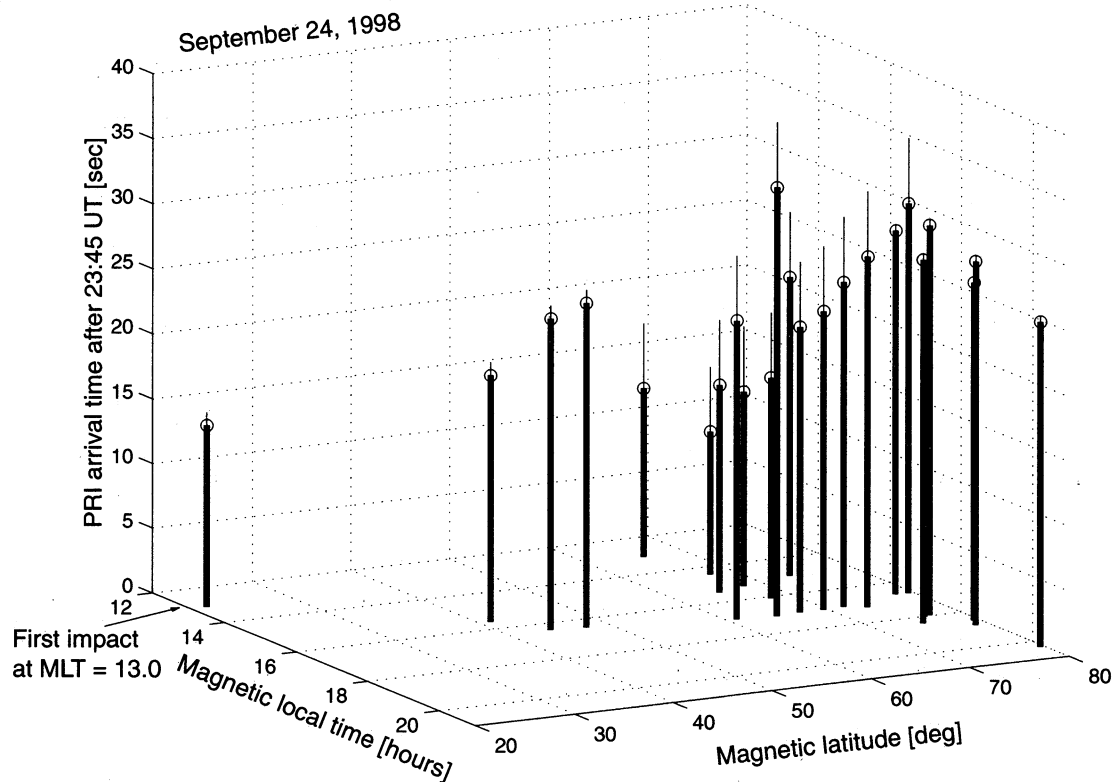


**Figure 6.** Arrival times of PRI observed at twenty-three magnetometer stations for the SC event on September 24, 1998. The sudden compression started at 12.3 magnetic local time. The thin line segments above the circles represent the uncertainty in determining the PRI arrival time due to the time resolution of the data.

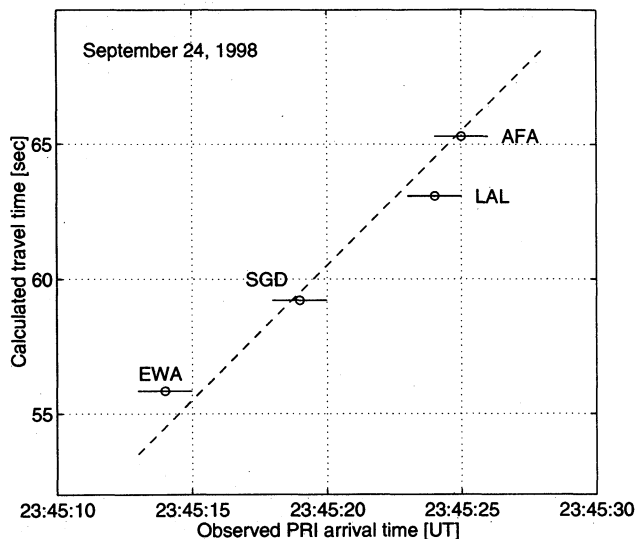


**Figure 7.** A comparison between the observed PRI arrival time and the calculated arrival time based on MHD wave propagation. The dashed line has a slope equal 1. The error bars are  $\pm 1$  s, indicating the uncertainty in determining the PRI arrival time due to the 1-s time resolution of the magnetometer data.

To compare the observed PRI arrival times at the four low-latitude stations synchronized by GPS signals, we calculated the total propagation time as in Figure 5 in the three-dimensional magnetosphere. Using the observed shock normal vector in the solar wind [Russell *et al.*, 2000] and the Petrinec and Russell magnetopause model [Petrinec and Russell, 1996], we estimated that the first impact on the magnetopause was located at (9.44, 2.47, 1.01)  $R_E$  in GSM coordinates. The Tsyganenko 1996 model [Tsyganenko, 1995, 1996] was included for tracing the field lines connected to the ground stations and calculating the magnetic field values along the shortest path from the impact point to the field line. Equation (1) was again used for the plasma density in the magnetosphere. The results are presented in Figure 7, where the observed PRI arrival times and the calculated travel times closely follow a straight line with a slope equal to 1. The agreement between the observations and the MHD wave propagation model is evident.

#### 4. Discussion

On the basis of the propagation of MHD waves, our result in Figure 5 can be used to interpret other similar phenomena in the magnetospheric system that share the same physics. In particular, the Pi2 phenomenon, considered as a consequence of the abrupt motion in the nighttime magnetosphere, may have a similar pattern for the arrival time on the Earth. Recently, Uozumi *et al.* [2000] presented the latitudinal dependence of the observed Pi2 arrival time consistent with their time-of-flight calculation analogous to the one in this study.

In essence, the “zigzag” shape of the travel time profile as shown in Figure 5 comes from the part of Alfvén wave propagation along the field line. A signal can save its travel time to the Earth by first traveling inwardly via the fast mode wave to a lower  $L$ , where the Alfvén speed is on average higher, and then propagating along the field line to the ionosphere. Our intuition tends to think the opposite way that the signal should arrive at a lower-latitude region later since it is farther from the external source. The slowdown of waves in the dense plasmasphere is

relatively well known, and some insightful illustration and simulations have been demonstrated by Wilken *et al.* [1982], Lee and Kim [2000], and Lee and Hudson [2001]. It should be noted here that the calculation in some early papers [e.g., Francis *et al.*, 1959] does not include a plasmasphere in their model. Overall, the wave front of the SC signal is highly distorted because of the strong diffraction in the magnetosphere.

A calculation of the MHD wave travel time from the impact location to different spacecraft for this SC event provides further support of the validity of our result in Figure 7. Russell *et al.* [1999] reported a sharp magnetic field increase observed by the GOES 10 geosynchronous satellite at 2344:53 UT and a compressional wave front seen by the Polar spacecraft above the polar cap at 2345:08 UT. Using the fitted line in Figure 7, we projected backward in time and estimated the time of the first impact on the magnetopause at 2344:20 UT. We then calculated the travel time in the Tsyganenko 1996 model field and obtained 32.1 and 48.4 s from the source location to GOES 10 and Polar, respectively, matching the arrival times reported by Russell *et al.* [1999] almost perfectly. We also found a very good agreement between the estimated arrival time of the compressional wave front and the FAST magnetic field observations reported by Strangeway *et al.* [2000].

The timing accuracy has been an important factor that influences the interpretation of PRI, both in the past and at present. The paradigm of the Earth-ionosphere waveguide propagation of PRI was built on the observational facts that the PRI onset was seen simultaneously at all locations, ranging from high-latitude regions to the equator. However, the timing accuracy of magnetometers at that time was not sufficient to identify the small time delays between the stations. As indicated by Yumoto *et al.* [1997], the data used by Araki [1977] and Araki *et al.* [1985] for verifying the instantaneous transmission of PRI had time accuracy not better than 10 s. Similarly, we are motivated to interpret PRI as MHD waves propagating from the impact location by having high-resolution magnetic field observations and observing the small time delays of PRI signals among the stations. Our analysis is, nevertheless, restricted by the incomplete synchronization across different magnetometer arrays. These facts suggest that a common synchronization scheme among ground magnetometers is of paramount importance in future observations of sudden commencements.

The unavailability of PRI observations at the equator in this SC event prevents us from assessing the MHD wave propagation model for equatorial PRIs. Almost the entire dayside equator was located in the Pacific Ocean. The South American station ANC, whose magnetic latitude is  $3.1^\circ$ , was located in the nightside and did not see a PRI. If the PRI signal travels to the equator also by means of MHD waves, our result in Figure 5 suggests that the arrival time would be slightly earlier than that at a low-latitude station, such as EWA in this study. Tamao [1964a] proposes that the westward electrojet current, driven by the westward electric field of the converted Alfvén wave, will flow within a narrow belt at the equator and produce a negative perturbation in  $B_H$ . He further estimated that this process may dominate over the increase of  $B_H$  associated with the compression mode. However, Kikuchi and Araki [1979a] also presented analytic calculations indicating that the direct incidence of MHD waves onto the equatorial ionosphere cannot produce the equatorial PRI. Further studies are needed to explore whether the equatorial PRI and the low-latitude counterparts as reported in this study share the same propagation mechanism or the equatorial PRI is attributed to the high-latitude PRI propagating through the Earth-ionosphere waveguide as suggested by Kikuchi and Araki [1979b].

Although the observations at low latitudes show good agreement with our calculation based on MHD wave propagation, we think that high-latitude PRIs require additional consideration

regarding the evolution of ionospheric currents associated with the compression of the magnetosphere. First, the PRI with an amplitude roughly 100 nT seen by MACCS magnetometers at cusp latitudes seems to have its causative ionospheric current located at a lower latitude. The Tsyganenko 1996 model suggests that the field lines connected to MACCS stations were extended either to the dusk side of the magnetosphere or to the magnetotail at the time of the SC event. The propagation path that preserves the most wave energy was roughly the straight-line path between the source and the ground station. If the same MHD wave propagation model in Figure 4 was still valid, the wave amplitudes would have been weaker than what were observed at low-latitude stations. Second, the evolution of the equivalent ionospheric currents as shown in Figure 3 seems to indicate a moving vortex during the SC event. At 2345:15 UT (Figure 3a) the currents generally directed to the southwest, which implies that the vortex center was in the west. Forty-five seconds later at 2346:00 UT (Figure 3b), the direction of currents changed to the northwest, meaning that the vortex center moved to the east. The westward component of these vectors again implies that the ionospheric currents were located below the cusp latitude. Third, if the uncertainty in synchronization between the MACCS magnetometers and the IGPP/LANL stations does not impose a serious problem, the high-latitude stations generally observed the minimum of  $B_H$  ~20 s later than the time when an Alfvén wave arrived at the Earth directly from the source. This delay is likely due to the motion of the ionospheric current vortex. The above consideration of the ionospheric current system is similar to what some early studies proposed to explain high-latitude PIs. In the review paper by Araki [1994], he mentioned the work by Osada [1992], who proposed a two-pair-field-aligned-current model that evolves with time. Engebretson et al. [1999] also postulated possible mechanisms generating the PI in the polar region, such as the short-lived field-aligned currents flowing down to the ionosphere at cusp/cleft latitudes on either side of local noon.

There may be some other missing pieces of information about PRI for further study. We would like to restate an interesting issue raised by Araki [1977] about the "pure SC" events, the SC events containing no PRI signatures. According to the statistics by Araki [1977], pure SC events occupy 25% of his database. However, a compression of the magnetosphere should always lead to an eastward current on the magnetopause, and it is not clear why Tamao's picture of twin vortices could not be projected on the ionosphere for the pure SC events. The answer may be related to the IMF effect on SC [e.g., Kokubun et al., 1977], which has not been a well-explored subject. A complete picture of PRIs should explain why they are not always seen.

Although we have not pursued this objective herein, the availability of accurately characterized interplanetary shocks and extensive arrays of high-resolution synchronized magnetometers on the ground now allows the equivalent of magnetic seismology of the magnetospheric plasma using the observed travel times. While the number of these GPS controlled sites is still small, the first steps at deriving the density of the hidden populations of the magnetospheric plasma can now be undertaken.

In summary, we found compelling evidence that low-latitude PRI signals are the MHD waves traveling through the magnetosphere from the location of the first magnetospheric compression to the ground. The difference in PRI arrival times can be as large as 30 s at different locations on the ground, and it can be distinguished by modern magnetometers with high timing resolution and synchronization. We found unambiguous differences in the PRI arrival time at different magnetometer stations for the SC event on September 24, 1998, and the time delays agree well with the MHD wave propagation pattern suggested by Tamao [1964b], but inconsistent with the Earth-ionosphere waveguide propagation at the speed of light. Our

calculation of the signal travel time also suggests that a PRI arrives at the station at a lower latitude sooner than at the station at a higher latitude, if both stations are located on the same meridian plane as the source. The PRI signal also suffers a slowdown in the plasmasphere, and as a result simultaneous observations of PRI at two different latitudes may not mean that the signal propagates at a super-Alfvénic speed. A high-latitude PRI can be induced by the strong ionospheric current at a slightly lower latitude, and the PRI arrival time may depend on the motion of the ionospheric vortices. Equatorial PRIs are not observed in this SC event, and their causes require further exploration.

**Acknowledgments.** We thank Mark Engebretson for providing MACCS magnetometer data. The CANOPUS instrument array constructed, maintained and operated by the Canadian Space Agency, provided the data used in this study. The MEASURE data were supported by NSF grant ATM-9628708. This study was supported by NASA NAG 5-7721 and LANL CULAR UC 98-202.

Michel Blanc thanks Mary Hudson and another referee for their assistance in evaluating this paper.

## References

- Araki, T., Global structure of geomagnetic sudden commencements, *Planet. Space Sci.*, **25**, 373-384, 1977.
- Araki, T., A physical model of the geomagnetic sudden commencement, in *Solar Wind Sources of Magnetospheric Ultra-Low-Frequency Waves*, *Geophys. Monogr. Ser.*, Vol. 81, edited by M. J. Engebretson et al., pp.183-200, AGU, Washington, D.C., 1994.
- Araki, T., J. H. Allen, and Y. Araki, Extension of a polar ionospheric current to the nightside equator, *Planet. Space Sci.*, **33**, 11-16, 1985.
- Chi, P. J., C. T. Russell, S. Musman, W. K. Peterson, G. Le, V. Angelopoulos, G. D. Reeves, M. B. Moldwin, and F. K. Chun, Plasmaspheric depletion and refilling associated with the September 25, 1998 magnetic storm observed by ground magnetometers at  $L = 2$ , *Geophys. Res. Lett.*, **27**, 633-636, 2000.
- Engebretson, M. J. et al., A multipoint determination of the propagation velocity of a sudden commencement across the polar ionosphere, *J. Geophys. Res.*, **104**, 22,433-22,451, 1999.
- Francis, W. E., M. I. Green, and A. J. Dessler, Hydromagnetic propagation of sudden commencements of magnetic storms, *J. Geophys. Res.*, **64**, 1643-1645, 1959.
- Hughes, W. J., and M. J. Engebretson, MACCS: Magnetometer array for cusp and cleft studies, in *Satellite-Ground Based Coordination Sourcebook*, edited by M. J. Lockwood et al., *Eur. Space Agency Spec. Publ.*, **SP-1198**, 119, 1997.
- Kikuchi, T., and T. Araki, Transient response of uniform ionosphere and preliminary reverse impulse of geomagnetic storm sudden commencement, *J. Atmos. Terr. Phys.*, **41**, 917-925, 1979a.
- Kikuchi, T., and T. Araki, Horizontal transmission of the polar electric field to the equator, *J. Atmos. Terr. Phys.*, **41**, 927-936, 1979b.
- Kokubun, S., R. L. McPherron, and C. T. Russell, Triggering of substorms by solar wind discontinuities, *J. Geophys. Res.*, **82**, 74-86, 1977.
- Lee, D.-H., and M. K. Hudson, Numerical studies on the propagation of sudden impulses in the dipole magnetosphere, *J. Geophys. Res.*, **106**, 8435-8445, 2001.
- Lee, D.-H., and K. Kim, Propagation of sudden impulses in the magnetosphere: Linear waves, *Adv. Space Res.*, **25**(7-8), 1531-1539, 2000.
- Lee, D.-H., and R. L. Lysak, Magnetospheric ULF wave coupling

- in the dipole model: The impulsive excitation, *J. Geophys. Res.*, *94*, 17,097-17,103, 1989.
- Lysak, R. L., and D.-H. Lee, Response of the dipole magnetosphere to pressure pulses, *Geophys. Res. Lett.*, *19*, 937-940, 1992.
- Moore, T. E., W. K. Peterson, C. T. Russell, M. O. Chandler, M. R. Collier, H. L. Collin, P. D. Craven, R. Fitzenreiter, B. L. Giles, and C. J. Pollock, Ionospheric mass ejection in response to a coronal mass ejection, *Geophys. Res. Lett.*, *26*, 2339-2342, 1999.
- Matsushita, S., On geomagnetic sudden commencements, sudden impulses, and storm durations, *J. Geophys. Res.*, *67*, 3753-3777, 1962.
- Nishida, A., Ionospheric screening effect and storm sudden commencement, *J. Geophys. Res.*, *69*, 1861-1874, 1964.
- Obayashi, T., and J. A. Jacobs, Sudden commencements of geomagnetic storms and atmospheric dynamo action, *J. Geophys. Res.*, *62*, 589-616, 1957.
- Osada, S., Numerical calculation of geomagnetic sudden commencement, Master's thesis, Fac. of Sci., Kyoto Univ., Kyoto, Japan, March 1992.
- Petrinec, S. M., and C. T. Russell, Near-Earth magnetotail shape and size as determined from the magnetopause flaring angle, *J. Geophys. Res.*, *101*, 137-152, 1996.
- Petrinec, S. M., K. Yumoto, H. Luhr, D. Orr, D. Milling, K. Hayashi, S. Kokubun, and T. Araki, The CME event of February 21, 1994: Response of the magnetic field at the Earth's surface, *J. Geomagn. Geoelectr.*, *48*, 1341, 1996.
- Russell, C. T., X. W. Zhou, P. J. Chi, H. Kawano, T. E. Moore, W. K. Peterson, J. B. Cladis, and H. J. Singer, Sudden compression of the outer magnetosphere associated with an ionospheric mass ejection, *Geophys. Res. Lett.*, *26*, 2343-2346, 1999.
- Russell, C. T. et al., The interplanetary shock of September 24, 1998: Arrival at Earth, *J. Geophys. Res.*, *105*, 25,143-25,154, 2000.
- Strangeway, R. J., C. T. Russell, C. W. Carlson, J. P. McFadden, R. E. Ergun, M. Temerin, D. M. Klumpar, W. K. Peterson, and T. E. Moore, Cusp field-aligned currents and ion outflows, *J. Geophys. Res.*, *105*, 21,129-21,142, 2000.
- Tamao, T., A hydromagnetic interpretation of geomagnetic SSC\*, *Rep. Ionos. Space Res. Jpn.*, *18*, 16-31, 1964a.
- Tamao, T., The structure of three-dimensional hydromagnetic waves in a uniform cold plasma, *J. Geomagn. Geoelectr.*, *18*, 89-114, 1964b.
- Tsyganenko, N. A., Modeling the Earth's magnetospheric magnetic field confined within a realistic magnetopause, *J. Geophys. Res.*, *100*, 5599-5612, 1995.
- Tsyganenko, N. A., Effects of the solar wind conditions on the global magnetospheric configuration as deduced from data-based field models, *Eur. Space Agency Spec. Publ.*, *ESA SP-389*, 181-185, 1996.
- Uozumi, T., K. Yumoto, H. Kawano, A. Yoshikawa, J. V. Olson, S. I. Solov'yev, and E. F. Vershinin, Characteristics of energy transfer of Pi 2 magnetic pulsations: Latitudinal dependence, *Geophys. Res. Lett.*, *27*, 1619-1622, 2000.
- Wilken, B., C. K. Goertz, D. N. Baker, P. R. Higbie, and T. A. Fritz, The SSC on July 29, 1977 and its propagation within the magnetosphere, *J. Geophys. Res.*, *87*, 5901-5910, 1982.
- Yumoto, K., and the 210 MM Magnetic Observation Group, The STEP 210° magnetic meridian network project, *J. Geomagn. Geoelectr.*, *48*, 1297-1309, 1996.
- Yumoto, K., V. Pilipenko, E. Fedorov, N. Kurneva, M. De Laetis, and K. Kitamura, Magnetospheric ULF wave phenomena stimulated by SSC, *J. Geomagn. Geoelectr.*, *49*, 1179-1195, 1997.

---

V. Angelopoulos, Space Science Laboratory, University of California, Grizzly Peak Blvd. at Centennial Dr., Berkeley, CA 94720, USA.

P. J. Chi, M. B. Moldwin, J. Raeder, and C. T. Russell, Institute of Geophysics and Planetary Physics, UCLA, Los Angeles, CA 90095, USA. (pchi@igpp.ucla.edu)

H. Kawano, K. Kitamura, and K. Yumoto, Department of Earth and Space Sciences, Kyushu University 33, 6-10-1 Hakozaki, Fukuoka 812-8581, Japan.

G. Le, Laboratory for Extraterrestrial Physics, NASA Goddard Space Flight Center, Greenbelt, MD 20771, USA.

S. M. Petrinec, Lockheed Martin Advanced Research Center, 3251 Hanover Street, Palo Alto, CA 94304, USA.

E. Zesta, Department of Atmospheric Sciences, UCLA, Los Angeles, CA 90095, USA.

(Received February 22, 2001; revised April 17, 2001; accepted April 17, 2001.)